

## ORIGINAL ARTICLE

# Middle East respiratory syndrome coronavirus M protein suppresses type I interferon expression through the inhibition of TBK1-dependent phosphorylation of IRF3

Pak-Yin Lui<sup>1,\*</sup>, Lok-Yin Roy Wong<sup>1,\*</sup>, Cheuk-Lai Fung<sup>1</sup>, Kam-Leung Siu<sup>1</sup>, Man-Lung Yeung<sup>2</sup>, Kit-San Yuen<sup>1</sup>, Chi-Ping Chan<sup>1</sup>, Patrick Chiu-Yat Woo<sup>2</sup>, Kwok-Yung Yuen<sup>2</sup> and Dong-Yan Jin<sup>1</sup>

Middle East respiratory syndrome coronavirus (MERS-CoV) infection has claimed hundreds of lives and has become a global threat since its emergence in Saudi Arabia in 2012. The ability of MERS-CoV to evade the host innate antiviral response may contribute to its severe pathogenesis. Many MERS-CoV-encoded proteins were identified to have interferon (IFN)-antagonizing properties, which correlates well with the reduced IFN levels observed in infected patients and *ex vivo* models. In this study, we fully characterized the IFN-antagonizing property of the MERS-CoV M protein. Expression of MERS-CoV M protein suppressed type I IFN expression in response to Sendai virus infection or poly(I:C) induction. This suppressive effect was found to be specific for the activation of IFN regulatory factor 3 (IRF3) but not nuclear factor- $\kappa$ B. MERS-CoV M protein interacted with TRAF3 and disrupted TRAF3–TBK1 association leading to reduced IRF3 activation. M proteins from MERS-CoV and SARS-CoV have three highly similar conserved N-terminal transmembrane domains and a C-terminal region. Using chimeric and truncation mutants, the N-terminal transmembrane domains of the MERS-CoV M protein were found to be sufficient for its inhibitory effect on IFN expression, whereas the C-terminal domain was unable to induce this suppression. Collectively, our findings suggest a common and conserved mechanism through which highly pathogenic MERS-CoV and SARS-CoV harness their M proteins to suppress type I IFN expression at the level of TBK1-dependent phosphorylation and activation of IRF3 resulting in evasion of the host innate antiviral response.

*Emerging Microbes and Infections* (2016) 5, e39; doi:10.1038/emi.2016.33; published online 20 April 2016

**Keywords:** innate antiviral response; IRF3 activation; MERS coronavirus; RIG-I-like receptors; type I interferons

## INTRODUCTION

Middle East respiratory syndrome coronavirus (MERS-CoV) was first identified in Saudi Arabia in September 2012 as a novel coronavirus that causes severe acute respiratory disease.<sup>1</sup> Since then, this virus has caused recurrent outbreaks in the Arabian Peninsula and has spread, occasionally, to other parts of the world.<sup>2–9</sup> According to the World Health Organization, 1626 laboratory-confirmed cases were reported between September 2012 and 7 January 2016 with 586 related deaths in 26 countries.<sup>10</sup> In particular, 186 people were infected and 36 were killed in one recent outbreak in South Korea.<sup>10</sup> MERS-CoV is classified into lineage C of *Betacoronavirus* and is most phylogenetically related to two bat coronaviruses, HKU4 and HKU5, providing insight on its evolutionary origin.<sup>11,12</sup>

MERS-CoV is a polycistronic positive-sense single-stranded RNA virus with a genome of ~30 Kb in size. The 5' most two-thirds of MERS-CoV genome encodes polyproteins 1a and 1ab, which are further cleaved to yield 16 non-structural proteins, whereas the 3' end

of the genome encodes several structural or lineage-specific proteins.<sup>13</sup> Upon infection, these proteins are expressed to facilitate viral replication and propagation in the host.<sup>14</sup> MERS-CoV infection has been widely reported to mildly induce type I interferons (IFNs), including IFN- $\alpha$  and - $\beta$ , in patients as well as in animal and cellular infection models.<sup>15–21</sup> This has been attributed to the IFN-antagonizing property of some MERS-CoV-encoded proteins, which directly perturb the host IFN production mechanisms,<sup>22–26</sup> lending support to the notion that MERS-CoV uses multiple strategies to evade the innate immune response.

In non-specialized epithelial cells as well as a subset of specialized immune cells that are susceptible to MERS-CoV infection,<sup>16,18,27</sup> type I IFN production is an important part of the host innate immune response and is initiated by ubiquitously expressed cytoplasmic viral sensors in the retinoic acid-inducible gene-I (RIG-I)-like receptor (RLR) family in response to the detection of viral pathogen-associated molecular patterns such as double-stranded RNA (dsRNA).<sup>28,29</sup>

<sup>1</sup>School of Biomedical Sciences, The University of Hong Kong, Pokfulam Hong Kong, China and <sup>2</sup>Department of Microbiology, The University of Hong Kong, Pokfulam, Hong Kong, China

\*These authors contributed equally to this work.

Correspondence: DY Jin

E-mail: dyjin@hku.hk

Received 13 November 2015; revised 5 January 2016; accepted 6 January 2016

Stimulated RLRs mobilize downstream signal transducers that lead to the activation of the transcription factors IFN regulatory factor 3 (IRF3) and nuclear factor- $\kappa$ B (NF- $\kappa$ B) that drive IFN- $\beta$  expression.<sup>28</sup> The transduction events within this signaling cascade are prone to negative regulation by many MERS-CoV proteins. In a comparative analysis of MERS-CoV structural and accessory proteins, it has been shown that M, ORF4a, ORF4b and ORF5 possess IFN-antagonizing properties.<sup>22</sup> We, and others, have characterized the ORF4a protein as a dsRNA-binding protein that interferes with the activation of RLR by either a dsRNA ligand or the protein co-activator PACT.<sup>24,25</sup> However, the molecular mechanisms through which other MERS-CoV proteins manipulate the RLR signaling pathway to disrupt IFN- $\beta$  expression have not been elucidated.

In this study, we focused on the characterization of the MERS-CoV M protein in IFN antagonism. Coronavirus M protein is a transmembrane glycoprotein localized predominantly to the Golgi complex and is required for virion assembly.<sup>30–32</sup> MERS-CoV M protein is of particular interest because SARS-CoV M protein also inhibits IFN production through a mechanism by which the formation of TRAF3-TANK-TBK1/IKK- $\epsilon$  complex is impeded to ablate the activation of IRF3 transcription factor.<sup>30</sup> In contrast, M protein encoded by human coronavirus HKU1 associated with common cold has no influence on IFN production.<sup>32</sup> Here we reported that the MERS-CoV M protein also specifically inhibited IRF3 activation but not NF- $\kappa$ B signaling. MERS-CoV M protein was capable of interacting with TRAF3 adapter protein and hampered TRAF3-TBK1 interaction leading to diminished IRF3 activation. Using a chimeric protein containing the MERS-CoV M protein N-terminal transmembrane domains and a dormant SARS-CoV M protein C-terminal domain, we confirmed that the N-terminal transmembrane domains of MERS-CoV M protein sufficiently account for its inhibitory effect. Although another chimera containing SARS-CoV M protein N-terminal transmembrane domains and a MERS-CoV M protein C-terminal domain was fully competent in IFN antagonism, a truncation mutant lacking the functional first transmembrane domain of SARS-CoV M was not, suggesting that the C-terminal domain of the MERS-CoV M protein is largely dispensable for its immunosuppressive activity.

## MATERIALS AND METHODS

### Plasmids

The IFN $\beta$ -luc reporter plasmid and RIG-I expression plasmid are gifts from Professor Takashi Fujita (Kyoto University, Kyoto, Japan).<sup>28</sup> The expression plasmids for TBK1, IRF3 and TRAF3 were generous gifts from Dr Genhong Cheng (University of California, Los Angeles, CA, USA),<sup>33,34</sup> whereas those for RIG-I N, IKK- $\epsilon$  and MAVS and I $\kappa$ B- $\alpha$  as well as IRF3-luc and  $\kappa$ B-luc reporter plasmids have been described elsewhere.<sup>30,35–37</sup>

Viral RNA was extracted from MERS-CoV-infected Vero-E6 cells. The M gene was PCR-amplified from complementary DNA and cloned into the *EcoRI/XhoI* sites of pCAGEN plasmid with the addition of a C-terminal V5-tag with the following primers: 5'-ATG TCT AAT ATG ACG CAA CTC ACT GA-3' (forward) and 5'-AGC TCG AAG CAA TGC AAG TTC-3' (reverse). The SARS-CoV M protein expression plasmid has been described elsewhere.<sup>30,32</sup> The expression plasmids for the SN and MN chimeras were constructed by assembly PCR with the following forward primers covering the breakpoints: 5'-AGG CTG TTT GCT CGT ACC CGC TCA TGG TGG TCA TTC AAT CCT GAG-3' (SN) and 5'-CCG GCT GTT TAT GAG AAC TGG ATC AAT GTG GTC ATT CAA CCC A-3' (MN). The reverse primers were complementary to their respective forward primers. The truncation mutant of the SN chimera lacking the first

transmembrane domain was constructed using the forward primer: 5'-ATG GTA ACA CTT GCT TGT TTT GTG CT-3'.

### Antibodies

Mouse anti-FLAG (M2) and anti- $\beta$ -actin antibodies were purchased from Sigma-Aldrich (St. Louis, MO, USA). Mouse anti-V5 and anti-HA (Y11) antibodies were purchased from Life Technologies (Grand Island, NY, USA) and Santa Cruz Biotechnology (Dallas, TX, USA), respectively. Rabbit anti-IRF3 and anti-phospho-IRF3 (Ser 386) antibodies were purchased from IBL-America (Minneapolis, MN, USA).

### Cell culture and Sendai virus

HEK-293 human embryonic kidney cells were maintained in Dulbecco's modified Eagle's medium with 10% fetal bovine serum (Life Technologies) at 37 °C in a humidified chamber supplemented with 5% carbon dioxide. Plasmid transfection was performed with GeneJuice (Merck Millipore; Billerica, MA, USA). poly(I:C) was purchased from Sigma-Aldrich and was transfected with Lipofectamine 2000 (Life Technologies). Sendai virus (Cantell strain) was purchased from American Type Culture Collection (Manassas, VA, USA).

### Reporter and protein assays

Dual-luciferase reporter assay, co-immunoprecipitation and western blotting were performed as previously described.<sup>30,38</sup> Particularly, relative luciferase activity in arbitrary units was calculated by normalizing firefly luciferase activity to *Renilla* luciferase activity recovered from cell lysate. Non-denaturing native polyacrylamide gel electrophoresis (PAGE) was performed as previously described.<sup>36,39,40</sup>

### Bioinformatic analysis

Sequence alignment was performed using Cluster Omega, an online tool based on the hidden Markov model,<sup>41</sup> and hosted by the EMBL-EBI server (<http://www.ebi.ac.uk/Tools/msa/clustalo/>). Transmembrane domain prediction was performed using TMFinder, which considers hydrophobicity and helicity of the amino-acid sequence (<http://tmfinder.research.sickkids.ca/>).<sup>42</sup>

## RESULTS

### Inhibition of IFN expression by MERS-CoV M protein mediated through IRF3

To characterize the MERS-CoV M protein in terms of its IFN antagonism, M protein was ectopically expressed in cultured cells for functional assays (Figure 1A). A luciferase reporter construct driven by IFN- $\beta$  promoter was used to reflect IFN- $\beta$  promoter activity stimulated during infection. Sendai virus was used as a model virus to potently induce IFN expression in transfected cells. When increasing doses of M proteins were expressed in advance, a dose-dependent inhibition of IFN- $\beta$  promoter activity was observed (Figure 1B; bars 3–5 compared with bar 2). A similar observation was also noted when synthetic dsRNA analog poly(I:C) was used as an alternative inducer that specifically stimulates the RLR pathway of IFN production (Figure 1C; bars 3–5 compared with bar 2). These two pieces of data are generally consistent with a previous report,<sup>22</sup> and they further strengthen the current model of the IFN antagonism of MERS-CoV M protein.

Cellular IFN- $\beta$  expression is under the control of multiple transcription factors, which work cooperatively to form a large enhanceosome complex.<sup>43</sup> In particular, IRF3 and NF- $\kappa$ B are two transcription factors that are primarily activated by RLR signaling.<sup>28,44,45</sup> MERS-CoV M protein has previously been shown to have no influence on NF- $\kappa$ B activation induced by Sendai virus infection.<sup>22</sup> However, it remains to be seen whether the MERS-CoV M

protein could preferentially inhibit IRF3 and NF- $\kappa$ B signaling after RIG-I activation. To address this issue, two different luciferase reporter constructs, in which tandem copies of either IRF3- or NF- $\kappa$ B-binding elements were inserted into their promoter region, were used. The truncation mutant of RIG-I known as RIG-I N that contains only the N-terminal CARD domain was chosen to be the inducer in these assays because it is constitutively active and highly competent to induce these two pathways.<sup>28</sup> The MERS-CoV M protein was able to suppress the promoter activity of the IRF3-driven luciferase construct in a dose-dependent manner (Figure 2A; bars 3–5 compared with bar 2), but no inhibitory effect was observed with the NF- $\kappa$ B-driven construct (Figure 2B; bars 3–5 compared with bar 2) although the canonical inhibitor I $\kappa$ B- $\alpha$  could efficiently blunt its activation as

a positive control (Figure 2B; bar 6 compared with bar 2). Hence, the suppressive effect of the MERS-CoV M protein is specific for IRF3 signaling but not NF- $\kappa$ B activation.

#### Inhibition of IRF3 activation by the MERS-CoV M protein at TRAF3–TBK1 level

To delineate the action point of the MERS-CoV M protein in IFN antagonism, we tested the ability of the M protein to inhibit the activation signal induced by different signal transducers of the RLR pathway individually. The activation signal will be mostly unaffected if the activation event mediated by that transducer is downstream of the action point where M protein exerts its inhibitory effect. As described above, RIG-I N is a constitutively active mutant that resembles

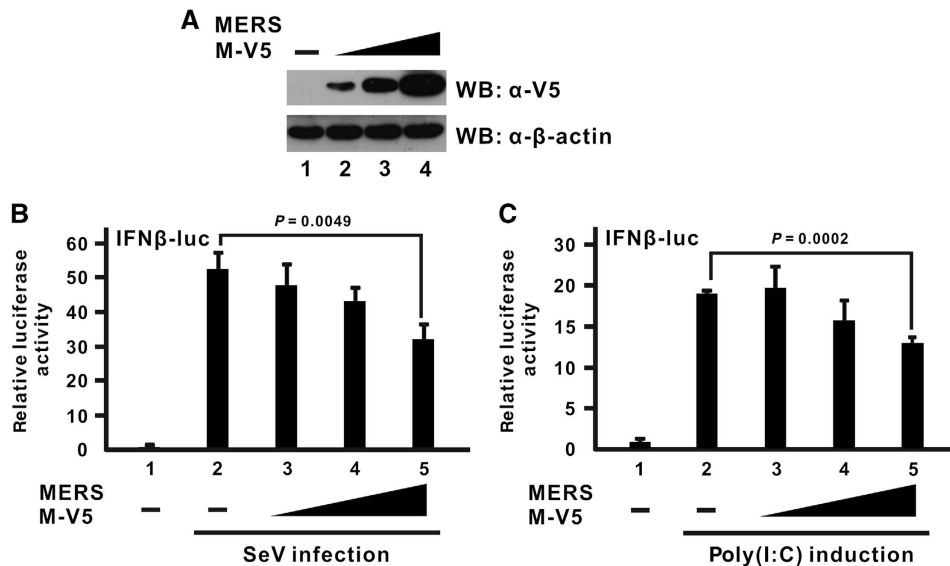


**Figure 1** MERS-CoV M protein inhibits IFN- $\beta$  expression stimulated by Sendai virus infection or poly(I:C) induction. Increasing doses of V5-tagged M protein expression plasmid (MERS M-V5) were transfected into HEK-293 cells. (A) Western blotting (WB) was performed with an anti-V5 antibody to confirm M protein expression in cell lysates.  $\beta$ -Actin was also used as an internal loading control. (B, C) M expression plasmid was co-transfected with a firefly luciferase reporter plasmid driven by the IFN- $\beta$  promoter (IFN $\beta$ -luc) and a control *Renilla* luciferase reporter plasmid. After 24 h, cells were challenged with either Sendai virus infection (SeV; 100 hemagglutinating units per mL) in B or poly(I:C) induction (1  $\mu$ L/mL) in C for 16 h before harvest for dual-luciferase reporter assay. Bars represent the mean of three biological replicates ( $n=3$ ) and error bars indicate their s.d. The statistical significance between selected samples was evaluated using a two-tailed Student's *t*-test for unpaired samples with equal variance and *P*-value (*P*) was indicated.

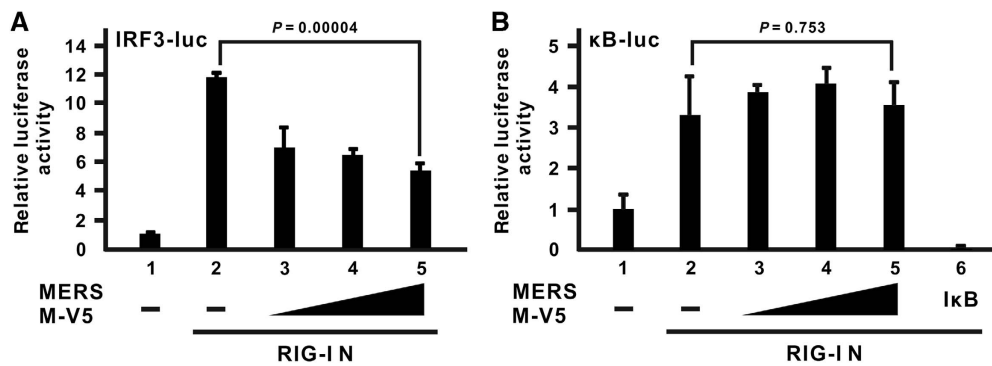


**Figure 2** MERS-CoV M protein suppresses IRF3 activation but not NF- $\kappa$ B signaling. An expression plasmid for dominant-active RIG-I N mutant containing the N-terminal domain of RIG-I alone was used as a potent IFN inducer and co-transfected with an M expression plasmid and a firefly luciferase plasmid driven by tandem copies of (A) IRF3-binding elements (IRF3-luc) or (B)  $\kappa$ B elements ( $\kappa$ B-luc) as well as the control *Renilla* luciferase plasmid. A canonical NF- $\kappa$ B inhibitor I $\kappa$ B- $\alpha$  (I $\kappa$ B) was included as a positive control for the inhibition of NF- $\kappa$ B activity. Cells were collected at 40 h post transfection for dual-luciferase reporter assay. Bars represent the mean of three biological replicates ( $n=3$ ) and error bars indicate their s.d. The statistical significance between selected samples was evaluated using a two-tailed Student's *t*-test for unpaired samples with equal variance and *P*-value (*P*) was indicated. retinoic acid-inducible gene-1, RIG-I.

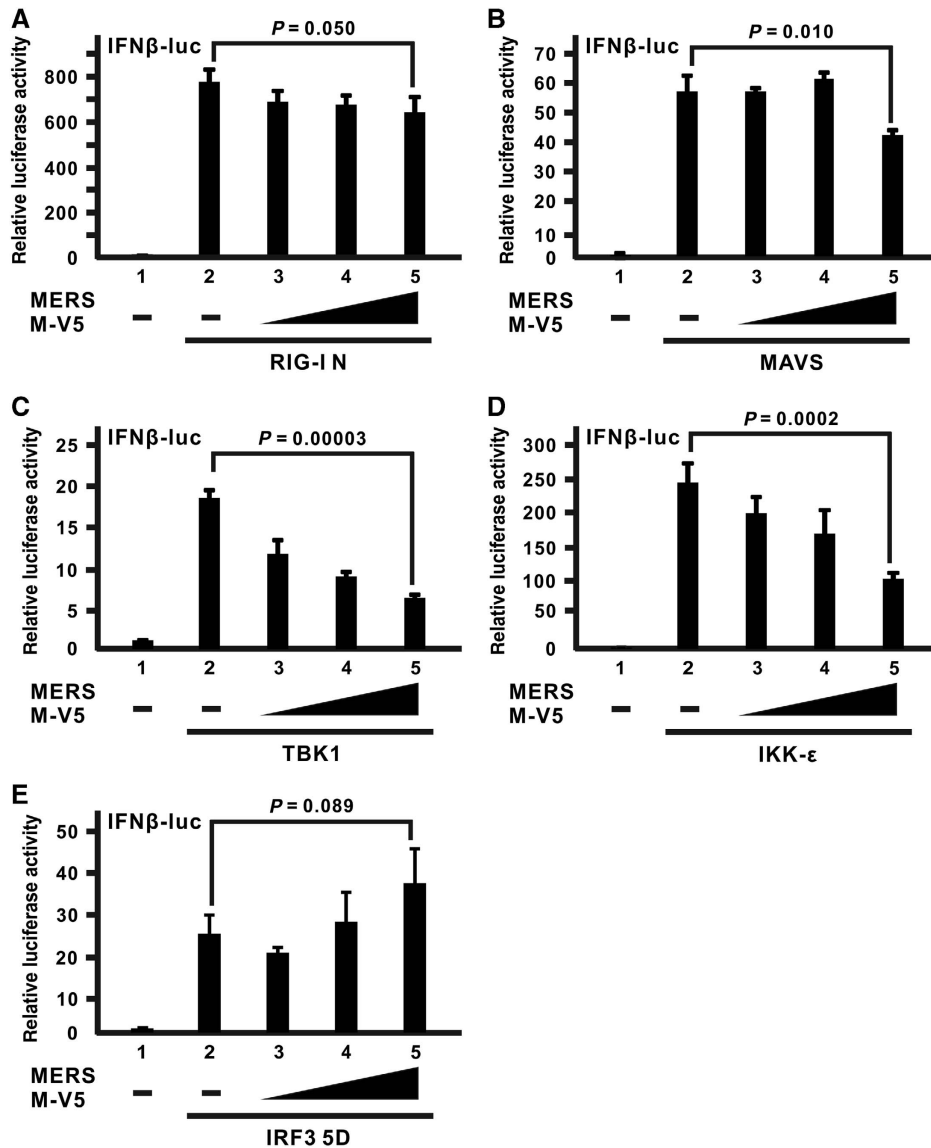


**Figure 3** The inhibitory effect of the MERS-CoV M protein occurs upstream of IRF3 activation. (A–E) HEK-293 cells were transfected with increasing doses of the MERS M-V5 expression plasmid, a firefly luciferase reporter plasmid driven by IFN- $\beta$  promoter (IFN $\beta$ -luc) and a control *Renilla* luciferase reporter plasmid, together with different expression plasmids of RLR pathway activators, RIG-I N in A, mitochondrial adapter MAVS in B, IRF3 kinases TBK1 and IKK- $\epsilon$  in C and D as well as a dominant-active IRF3 mutant (IRF3 5D) in E. Cells were collected after 40 h for dual-luciferase reporter assay. Bars represent the mean of three biological replicates ( $n=3$ ) and error bars indicate their s.d. The statistical significance between selected samples was evaluated using a two-tailed Student's *t*-test for unpaired samples with equal variance and *P*-value (*P*) was indicated. Retinoic acid-inducible gene-1, RIG-I; RIG-I-like receptor, RLR.

immediate activation of virus sensor RIG-I after the detection of viral infection. Although the M protein could mildly suppress IFN- $\beta$  promoter activation induced by RIG-I N at a marginally significant level, a dose-dependent effect was coarsely observed (Figure 3A; bars 3–5 compared with bar 2). A similar result was also obtained using MAVS as an activator (Figure 3B; bars 3–5 compared with bar 2), which is a mitochondrial adapter that diverts the activation signal from RIG-I to the IRF3 and NF- $\kappa$ B pathways.<sup>44–47</sup> When activators committed to the IRF3 pathway were used, greater inhibitory effects were observed, as in the cases of TBK1 (Figure 3C; bars 3–5 compared with bar 2) and IKK- $\epsilon$  (Figure 3D; bars 3–5 compared with bar 2), which are kinases which recognize and phosphorylate IRF3 as direct substrate.<sup>48–51</sup> Surprisingly, when a constitutively active mutant of IRF3 transcription factor (IRF3 5D), with five inducible phosphorylation

sites at Ser/Thr residues mutated to Asp,<sup>52</sup> was employed, the expression of the M protein no longer quenched the IRF3-induced activation of IFN- $\beta$  promoter (Figure 3E), suggesting that the inhibitory effect of M protein occurs upstream of IRF3 activation.

To further analyze the molecular mechanism and consequences through which MERS-CoV M protein exerts its inhibitory effect, we first investigated what signal transducer molecule might interact with the M protein. Several RLR transducers were ectopically expressed with MERS-CoV M protein in cultured cells for a co-immunoprecipitation experiment. When the transducers were precipitated with an anti-FLAG antibody, the M protein was only detected in TRAF3-containing precipitate (Figure 4A; lane 4 compared with lanes 1–3) even though M protein was abundantly expressed in all samples with other transducers (Figure 4A; lower panel for input),

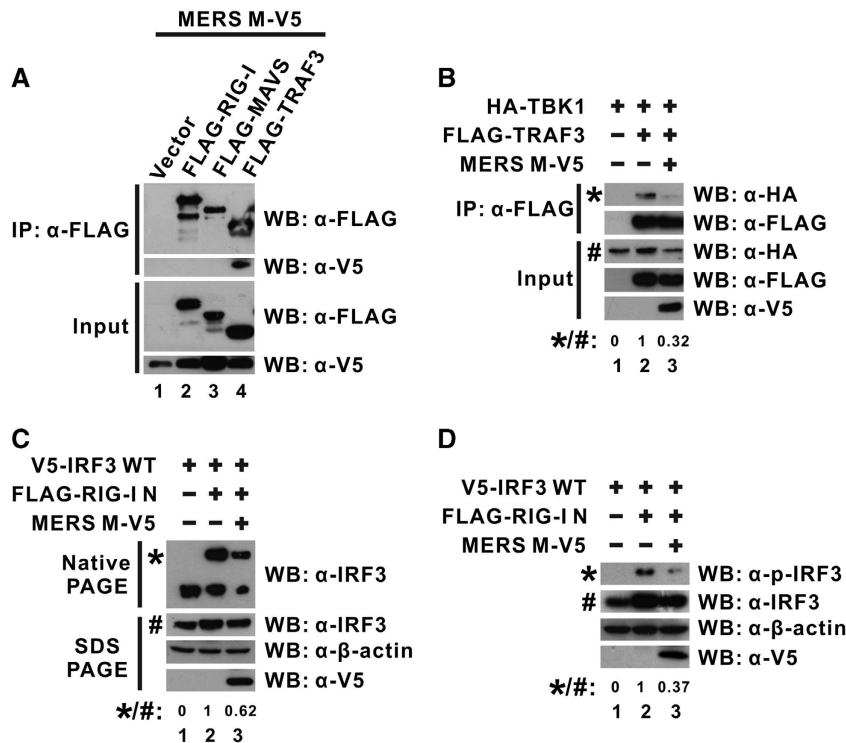


**Figure 4** MERS-CoV M protein binds with TRAF3 adapter and perturbs TRAF3–TBK1 interaction. **(A)** HEK-293 cells were transfected with plasmids expressing MERS M-V5 protein and different FLAG-tagged wild-type RLR pathway activators (FLAG-RIG-I, -MAVS and -TRAF3). An empty vector was used as a negative control in lane 1. Cells were collected after 40 h for a co-immunoprecipitation experiment with anti-FLAG antibody. The bound fraction of immunoprecipitates (IP) as well as total cell lysate (as input) were analyzed by western blotting (WB) with anti-FLAG and anti-V5 antibodies. **(B)** HEK-293 cells were transfected with different combinations of expression plasmids for MERS M-V5, FLAG-tagged TRAF3 and HA-tagged TBK1, and collected after 40 h for co-immunoprecipitation experiment with an anti-FLAG antibody to assay for TBK1 recruitment using an anti-HA antibody. **(C, D)** HEK-293 cells were transfected with different combinations of expression plasmids for wild-type IRF3, RIG-I N, and MERS M-V5. After 40 h, IRF3 dimerization from cell lysates was visualized by non-denaturing native PAGE followed by western blotting with anti-IRF3 antibodies **(C)**. IRF3 phosphorylation was also probed with anti-phospho-IRF3 antibodies **(D)**. The expression level of the ectopically expressed proteins was also individually verified in denaturing SDS-PAGE with respective antibodies. The relative band intensity (\*/#) of co-immunoprecipitated TBK1 in B, dimeric IRF3 in C or phospho-IRF3 (p-IRF3) in D for each sample was measured using ImageJ software. Retinoic acid-inducible gene-1, RIG-I; RIG-I-like receptor, RLR.

indicating the physical association between MERS-CoV M protein and TRAF3.

TRAF3 functions as an adapter that bridges the mitochondrial transducer MAVS with the downstream signaling complex containing TBK1 and IKK- $\epsilon$  kinases that are essential for IRF3 activation.<sup>34,53</sup> The physical association of the MERS-CoV M protein with TRAF3 (Figure 4A) prompted us to test whether the adapter function of TRAF3 would be particularly affected by M protein. We performed another co-immunoprecipitation experiment to explore the possibility that M protein could perturb the interaction of TRAF3 with the downstream transducer complex. When TRAF3 and TBK1 were ectopically expressed in cultured cells, the detection of TBK1 in TRAF3-immunoprecipitate confirmed the specific recruitment of TBK1 to TRAF3 in the absence of M protein (Figure 4B; lane 2 compared with lane 1). However, when M protein was added to the system, the interaction between TRAF3 and TBK1 was significantly disrupted (Figure 4B; lane 3 compared with lane 2), demonstrating that the physical association of MERS-CoV M protein with TRAF3 perturbs TRAF3–TBK1 interaction.

It was observed that MERS-CoV M protein disrupted TRAF3–TBK1 interaction (Figure 4B), which is required for IRF3 activation. We then evaluated whether IRF3 activation would be affected by the expression of M protein. IRF3 dimerization visualized by non-denaturing native PAGE is a sensitive assay for evaluating direct IRF3 activation.<sup>39</sup>

Therefore, we ectopically expressed IRF3 and M protein with the inducer RIG-I N in cultured cells and subjected cell lysates directly to native PAGE to check for IRF3 dimerization. When the inducer RIG-I N was exclusively co-expressed with IRF3, the detection of an additional slow-migrating band indicated the activation and dimerization of IRF3, which would otherwise be entirely in its monomeric form in the absence of any activator (Figure 4C; lane 2 compared with lane 1). Interestingly, when M protein was expressed, the signal reflecting the dimeric form of IRF3 molecules was significantly diminished, even though the total IRF3 level expressed in all samples was highly comparable as detected by conventional denaturing SDS-PAGE (Figure 4C; lower panel for SDS-PAGE), suggesting that IRF3 activation was greatly inhibited by the MERS-CoV M protein. IRF3 phosphorylation was also suppressed with the expression of MERS M protein in a similar experimental setup (Figure 4D; lane 3 compared with lane 2). Together with other results, MERS-CoV M protein was thought to interact with TRAF3 to perturb TRAF3–TBK1 interaction, which, in turn, affects IRF3 phosphorylation and activation.

#### Requirement and sufficiency of the N-terminal transmembrane domains of MERS-CoV M protein for its innate immunosuppressive effect

Given that the M proteins of both SARS-CoV and MERS-CoV were capable of antagonizing IFN production through highly similar



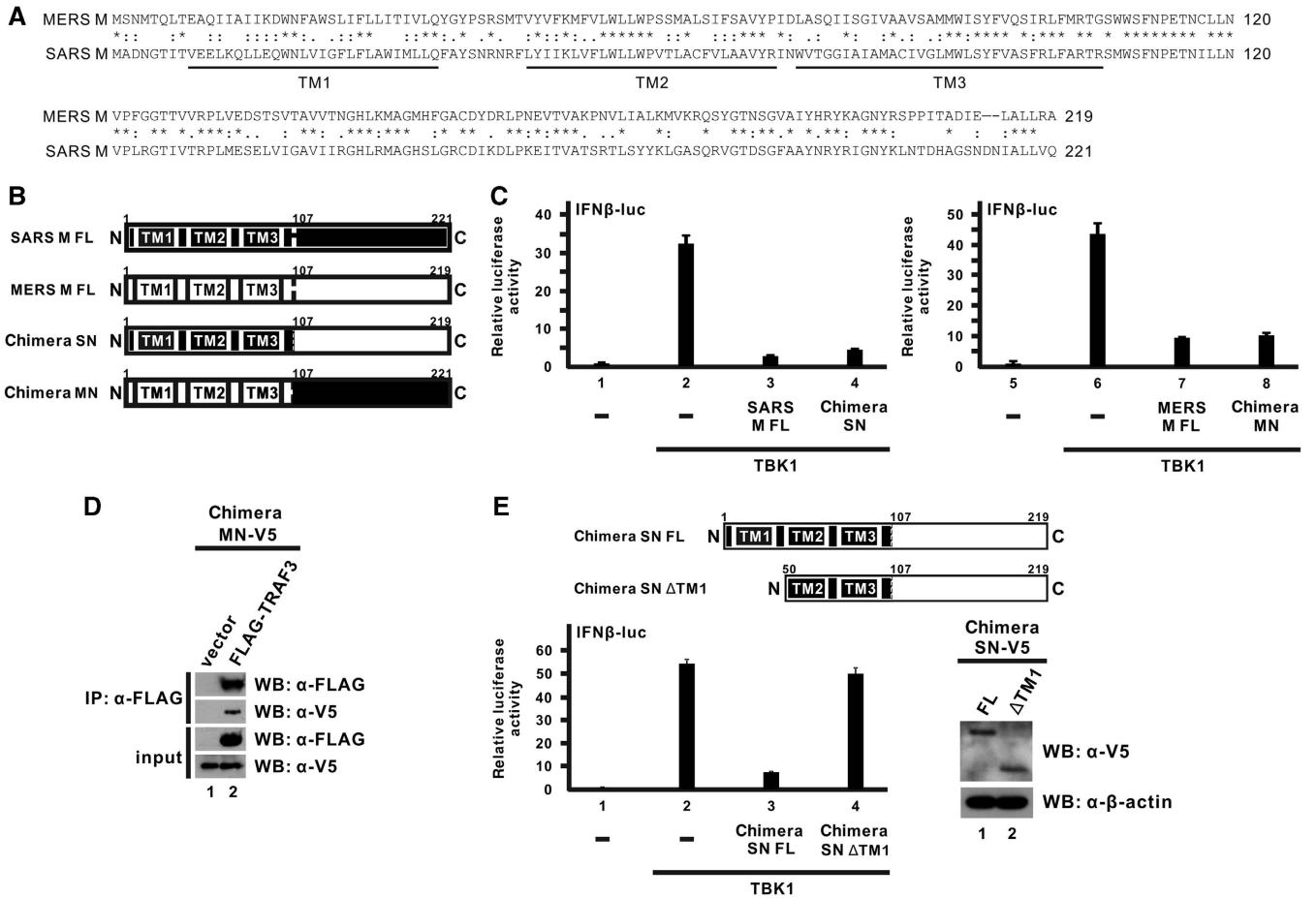


**Figure 5** The N-terminal transmembrane domains of the MERS-CoV M protein are sufficient for while its C-terminal domain is devoid of the innate immunosuppressive effect. (A) Sequence alignment of MERS-CoV and SARS-CoV M proteins. An asterisk (\*) denotes identical residues. A colon (:) and a period (.) represent amino acids with highly and weakly similar physicochemical properties, respectively. The three predicted transmembrane (TM1-3) domains are indicated below the sequences. (B) Diagrammatic representation of full-length MERS-CoV and SARS-CoV M proteins (MERS M-FL and SARS M-FL) as well as two chimeras (SN and MN) constructed by swapping the N-terminal and C-terminal domains of the two M proteins with each other. The predicted transmembrane domains and the residue numbers at the breakpoints are indicated. (C) HEK-293 cells were co-transfected with plasmids expressing the indicated chimeric protein or the respective full-length M protein together with a TBK1 expression plasmid, a firefly luciferase reporter plasmid driven by IFN- $\beta$  promoter (IFN $\beta$ -luc) and a control *Renilla* luciferase reporter plasmid. Cells were collected after 40 h for dual-luciferase reporter assay. Bars represent the mean of three biological replicates ( $n=3$ ) and error bars indicate their s.d. (D) HEK-293 cells were transfected with plasmids expressing V5-MN and FLAG-TRAF3 proteins. An empty vector was used as a negative control in lane 1. Cells were collected after 40 h for a co-immunoprecipitation experiment with an anti-FLAG antibody. The bound fraction of immunoprecipitates (IP) as well as total cell lysate (as input) were analyzed by western blotting (WB) with anti-FLAG and anti-V5 antibodies. (E) Diagrammatic representation of chimeric SN full-length (FL) protein and TM1-deletion ( $\Delta$ TM1) truncation mutant in the upper panel. Inhibition of IFN- $\beta$  promoter activity by chimeric SN FL or  $\Delta$ TM1 proteins was measured by luciferase reporter assay in the bottom-left panel as in C. The expression levels of these two proteins were visualized with anti-V5 antibody.  $\beta$ -Actin was also probed as an internal loading control in the bottom-right panel.

mechanisms,<sup>30</sup> it will be of interest to analyze the sequence and domain architecture of the two proteins. Sequence alignment of SARS-CoV and MERS-CoV M proteins revealed a strikingly high sequence similarity (> 70%) and the presence of three transmembrane domains at the N-termini (Figure 5A). According to the prediction results, we have initially constructed two truncation mutants for MERS-CoV M protein, an N-terminal transmembrane domain-containing mutant and a C-terminal mutant, and tested their inhibitory capacity in suppressing IFN- $\beta$  expression using a luciferase reporter assay. However, neither exhibited an inhibitory effect (data not shown), possibly due to unstable expression or aberrant localization.

To overcome the inactivity of truncation mutants and to define the inhibitory activity of different domains, we decided to create chimeric proteins using domain swapping between MERS-CoV and SARS-CoV

M proteins. Particularly, the SN chimera contains the N-terminal transmembrane domains from SARS-CoV M protein and the C-terminal domain from MERS-CoV M protein, whereas the MN chimera contains the N-terminal transmembrane domains from the MERS-CoV M protein and the C-terminal domain from the SARS-CoV M protein (Figure 5B). The breakpoint was designed to occur immediately after the third predicted transmembrane domain at residue 106 and before the conserved Ser residue in both proteins at residue 107 (Figure 5B).

We next compared the inhibitory effect of these two chimeras and the full-length M proteins on IFN- $\beta$  expression using the luciferase reporter assay. Our previous study showed that the IFN-antagonizing activity of the SARS-CoV M protein is mediated by its N-terminal transmembrane domains, but the C-terminal domain has no effect.<sup>32</sup>

When we swapped the C-terminal domain of the SARS-CoV M protein with that of the MERS-CoV M protein in the SN chimera, a similar suppressive effect on IFN- $\beta$  promoter activity was observed (Figure 5C; bar 4 compared with bar 3), consistent with our previous results.<sup>32</sup> Likewise, when we swapped the C-terminal domain of MERS-CoV M with that of SARS-CoV M protein in MN, the chimera was capable of suppressing IFN- $\beta$  promoter activity to comparable level (Figure 5C; bar 8 compared with bar 7). Given that the C-terminal domain of SARS-CoV M protein possesses no suppressive effect,<sup>32</sup> the inhibitory activity of the MN chimera would be predominantly due to the N-terminal domains of MERS-CoV M protein. A biochemical assay also confirmed that the MN chimera maintained the ability to interact with the TRAF3 adapter protein in a co-immunoprecipitation experiment (Figure 5D; lane 2 compared with lane 1). Therefore, we concluded that the N-terminal transmembrane domains of the MERS-CoV M protein are required and sufficient for its innate immunosuppressive activity.

To further determine whether the C-terminal domain of the MERS M protein also possesses IFN-antagonizing activity, we utilized the knowledge that the first transmembrane domain of SARS-CoV M protein is fully responsible for its suppression effect<sup>32</sup> to construct a truncation mutant lacking the first transmembrane domain in the SN chimera and tested its effect on IFN- $\beta$  expression using the luciferase reporter assay. This truncation mutant, designated SN  $\Delta$ TM1, contains only the second and the third transmembrane domains of SARS-CoV M protein at the N terminus fused with the C-terminal domain of MERS-CoV M protein (Figure 5E; upper panel). While the full-length chimeric SN protein was fully competent in suppressing IFN- $\beta$  promoter activity induced by TBK1, the removal of the first transmembrane domain of SARS-CoV M largely abolished its inhibitory capability (Figure 5E; bottom-left panel, bar 4 compared with bar 3), although both proteins were expressed to a detectable level in cells (Figure 5E; bottom-right panel). It is therefore proposed that the C-terminal domain of MERS-CoV M protein is devoid of and largely dispensable for the IFN-antagonizing activity of MERS-CoV M protein.

## DISCUSSION

In this study, we reported that the MERS-CoV M protein inhibited IRF3 activation, hence IFN expression, by disrupting TRAF3-TBK1 interaction. This innate immunosuppressive activity of the MERS-CoV M protein was due to its conserved N-terminal transmembrane domains. Our mechanistic study complemented the previous work that showed that MERS-CoV M protein had IFN-antagonizing activity.<sup>22</sup> Both studies demonstrated that MERS-CoV M protein suppressed IRF3 activity but not NF- $\kappa$ B signaling. It is known that the activation of RIG-I and MAVS results in the activation of both IRF3 and NF- $\kappa$ B.<sup>28,44–46</sup> Our results indicated that the MERS-CoV M protein was capable of differentially suppressing the RIG-I-induced activation of IRF3 (Figure 2). This provides further support to the bifurcation of IRF3 and NF- $\kappa$ B signaling subsequent to RIG-I and MAVS activation. Further investigations should elucidate the mechanism by which the MERS-CoV M protein preferentially modulates IRF3 activators such as TBK1, while sparing NF- $\kappa$ B activators such as CARD9.<sup>47</sup> We provided evidence that the TRAF3-TBK1 interaction as well as IRF3 phosphorylation and dimerization were affected by the MERS-CoV M protein (Figure 4). Our findings fill the knowledge gap by providing novel mechanistic insight into the innate immunosuppressive activity of MERS-CoV M protein.

In our study, TRAF3 was also shown to interact with the MERS-CoV M protein (Figure 4A). In line with this, the adapter function of

TRAF3 in TBK1 recruitment and subsequent IRF3 activation was perturbed by MERS-CoV M protein (Figures 4B–D), which plausibly contributed to the IFN antagonism of the MERS-CoV M protein (Figures 1–3). The MERS-CoV M protein is a transmembrane protein that was shown to co-localize with markers of the Golgi apparatus and endoplasmic reticulum (ER)–Golgi intermediate compartments in the perinuclear area.<sup>22</sup> Although TRAF3 is known to adapt the mitochondrial transducer MAVS, it is not associated with mitochondria but rather with the Golgi apparatus and ER–Golgi intermediate compartments in unstimulated conditions,<sup>30,54</sup> rendering it susceptible to interaction with the MERS-CoV M protein. Upon stimulation with ligands or viral infection, TRAF3 appears on membrane-bound fragments originating from Golgi. Retention of TRAF3 in ER-to-Golgi compartments and inability to form Golgi fragments rendered IFN- $\beta$  expression inefficient.<sup>54</sup> Therefore, whether TRAF3-containing Golgi fragment formation is affected by MERS-CoV M protein warrants further analysis. This may serve as a novel mechanism by which virus-encoded proteins counteract host IFN production.

MERS-CoV and SARS-CoV are two highly pathogenic coronaviruses that have caused hundreds of deaths. On one hand, the development of relevant prophylactic and therapeutic agents has been well under way.<sup>55–57</sup> On the other hand, the identification of the pathogenic factors in these viruses is also in full swing. The M protein is a pathogenic factor by virtue of its IFN-antagonizing property. Both the MERS-CoV and SARS-CoV M proteins were found to suppress IFN production with a highly similar mechanism in which the IRF3-phosphorylating complex of TRAF3-TANK-TBK1/IKK- $\epsilon$  was affected by their N-terminal transmembrane domains.<sup>30,32</sup> Interestingly, in the case of community-acquired human coronavirus HKU1, which normally causes common cold in infected individuals, its M protein showed no IFN antagonistic property,<sup>32</sup> further supporting the importance of the M protein in SARS-CoV and MERS-CoV pathogenesis. Using a side-by-side comparison of SARS-CoV and MERS-CoV M proteins, we discovered that the extent by which the MERS-CoV M protein suppressed IFN- $\beta$  promoter activity was lower than that by SARS-CoV M protein. This difference might be explained by the strengths of the interaction of MERS-CoV M protein with other transducers. Whereas the MERS-CoV M protein was found to be strongly associated with TRAF3, its interaction with TBK1 or IKK- $\epsilon$  was undetectable (data not shown). This distinguished MERS-CoV M protein from the SARS-CoV M protein, which interacts potently with every component of the TRAF3-TANK-TBK1/IKK- $\epsilon$  complex.<sup>30</sup> Further investigations are required to shed light on how the interaction of the M protein with TRAF3 complex might influence MERS-CoV pathogenesis.

Coronaviruses encode multiple proteins to counteract the host innate antiviral response.<sup>58–60</sup> MERS-CoV is no exception. Several MERS-CoV-encoded proteins have been identified to be IFN antagonists. We, and others, have characterized at least three IFN-antagonizing proteins encoded by MERS-CoV. In addition to the M protein reported in this study, ORF4a is a dsRNA-binding protein, which directly inhibits RLR activation induced by dsRNA and/or the protein co-activator PACT.<sup>24,25</sup> In addition, our unpublished data also revealed that ORF4b is a potent IFN antagonist. This is in line with findings by other groups although the mechanistic details of its action have not well documented.<sup>22,23</sup> One recent report suggested that ORF4b might not only interact directly with TBK1/IKK $\epsilon$  in the cytoplasm but also perturb IFN production in the nucleus through an as yet unknown mechanism.<sup>61</sup> Nevertheless, how M, ORF4a, ORF4b and the other IFN-antagonizing proteins of MERS-CoV coordinate with each other to modulate the host innate antiviral response to facilitate viral replication and propagation remains elusive.

## ACKNOWLEDGEMENTS

We thank Ron Fouchier (Erasmus Medical Center, Rotterdam, The Netherlands) for providing MERS-CoV isolate hCoV-EMC/2012; Genhong Cheng (University of California, Los Angeles, CA, USA) and Takashi Fujita (Kyoto University, Kyoto, Japan) for sharing constructs; and Hinson Cheung, Kitty Fung and Edwin Kong (The University of Hong Kong, Pokfulam, Hong Kong, China) for reading the manuscript critically. This work was supported by Hong Kong Health and Medical Research Fund (13121032, 14130822 and HKM-15-M01) and Hong Kong Research Grants Council (HKU1/CRF/11G, C7011-15R and T11-707/15-R).

- Zaki AM, van Boheemen S, Bestebroer TM, Osterhaus AD, Fouchier RA. Isolation of a novel coronavirus from a man with pneumonia in Saudi Arabia. *N Engl J Med* 2012; **367**: 1814–1820.
- Centers for Disease Control and Prevention (CDC). Severe respiratory illness associated with a novel coronavirus-Saudi Arabia and Qatar, 2012. *MMWR Morb Mortal Wkly Rep* 2012; **61**: 820.
- Bermingham A, Chand MA, Brown CS *et al*. Severe respiratory illness caused by a novel coronavirus, in a patient transferred to the United Kingdom from the Middle East, September 2012. *Euro Surveill* 2012; **17**: 20290.
- Mailles A, Blanckaert K, Chaud P *et al*. First cases of Middle East Respiratory Syndrome Coronavirus (MERS-CoV) infections in France, investigations and implications for the prevention of human-to-human transmission, France, May 2013. *Euro Surveill* 2013; **18**: 20502.
- Puzelli S, Azzi A, Santini MG *et al*. Investigation of an imported case of Middle East Respiratory Syndrome Coronavirus (MERS-CoV) infection in Florence, Italy, May to June 2013. *Euro Surveill* 2013; **18**: 20564.
- Tsiodras S, Baka A, Mentis A *et al*. A case of imported Middle East Respiratory Syndrome coronavirus infection and public health response, Greece, April 2014. *Euro Surveill* 2014; **19**: 20782.
- Bialek SR, Allen D, Alvarado-Ramy F *et al*. First confirmed cases of Middle East respiratory syndrome coronavirus (MERS-CoV) infection in the United States, updated information on the epidemiology of MERS-CoV infection, and guidance for the public, clinicians, and public health authorities - May 2014. *MMWR* 2014; **63**: 431–436.
- Chan JF, Lau SK, To KK, Cheng VC, Woo PC, Yuen KY. Middle East respiratory syndrome coronavirus: another zoonotic betacoronavirus causing SARS-like disease. *Clin Microbiol Rev* 2015; **28**: 465–522.
- Hui DS, Perlman S, Zumla A. Spread of MERS to South Korea and China. *Lancet Respir Med* 2015; **3**: 509–510.
- World Health Organization (WHO). Middle East respiratory syndrome coronavirus (MERS-CoV), 2015. WHO: Geneva, 2015. Available at <http://www.who.int/emergencies/mers-cov/en> (accessed 5 November 2015).
- de Groot RJ, Baker SC, Baric RS *et al*. Middle East respiratory syndrome coronavirus (MERS-CoV): announcement of the Coronavirus Study Group. *J Virol* 2013; **87**: 7790–7792.
- Lu L, Liu Q, Du L, Jiang S. Middle East respiratory syndrome coronavirus (MERS-CoV): challenges in identifying its source and controlling its spread. *Microbes Infect* 2013; **15**: 625–629.
- van Boheemen S, de Graaf M, Lauber C *et al*. Genomic characterization of a newly discovered coronavirus associated with acute respiratory distress syndrome in humans. *MBio* 2012; **3**: e00473–e00512.
- Durai P, Batool M, Shah M, Choi S. Middle East respiratory syndrome coronavirus: transmission, virology and therapeutic targeting to aid in outbreak control. *Exp Mol Med* 2015; **47**: e181.
- Zielecki F, Weber M, Eickmann M *et al*. Human cell tropism and innate immune system interactions of human respiratory coronavirus EMC compared to those of severe acute respiratory syndrome coronavirus. *J Virol* 2013; **87**: 5300–5304.
- Chan RW, Chan MC, Agnihotram S *et al*. Tropism of and innate immune responses to the novel human betacoronavirus lineage C virus in human ex vivo respiratory organ cultures. *J Virol* 2013; **87**: 6604–6614.
- Lau SK, Lau CC, Chan KH *et al*. Delayed induction of proinflammatory cytokines and suppression of innate antiviral response by the novel Middle East respiratory syndrome coronavirus: implications for pathogenesis and treatment. *J Gen Virol* 2013; **94**: 2679–2690.
- Zhou J, Chu H, Li C *et al*. Active replication of Middle East respiratory syndrome coronavirus and aberrant induction of inflammatory cytokines and chemokines in human macrophages: implications for pathogenesis. *J Infect Dis* 2014; **209**: 1331–1342.
- Faure E, Poissy J, Goffard A *et al*. Distinct immune response in two MERS-CoV-infected patients: can we go from bench to bedside? *PLoS One* 2014; **9**: e88716.
- Chan JF, Yao Y, Yeung ML *et al*. Treatment With Lopinavir/Ritonavir or interferon- $\beta$  improves outcome of MERS-CoV infection in a nonhuman primate model of common marmoset. *J Infect Dis* 2015; **212**: 1904–1913.
- Agrawal AS, Garron T, Tao X *et al*. Generation of a transgenic mouse model of Middle East respiratory syndrome coronavirus infection and disease. *J Virol* 2015; **89**: 3659–3670.
- Yang Y, Zhang L, Geng H *et al*. The structural and accessory proteins M, ORF 4a, ORF 4b, and ORF 5 of Middle East respiratory syndrome coronavirus (MERS-CoV) are potent interferon antagonists. *Protein Cell* 2013; **4**: 951–961.
- Matthews KL, Coleman CM, van der Meer Y, Snijder EJ, Frieman MB. The ORF4b-encoded accessory proteins of Middle East respiratory syndrome coronavirus and two related bat coronaviruses localize to the nucleus and inhibit innate immune signalling. *J Gen Virol* 2014; **95**: 874–882.
- Niemeyer D, Zillinger T, Muth D *et al*. Middle East respiratory syndrome coronavirus accessory protein 4a is a type I interferon antagonist. *J Virol* 2013; **87**: 12489–12495.
- Siu KL, Yeung ML, Kok KH *et al*. Middle east respiratory syndrome coronavirus 4a protein is a double-stranded RNA-binding protein that suppresses PACT-induced activation of RIG-I and MDA5 in the innate antiviral response. *J Virol* 2014; **88**: 4866–4876.
- Yang X, Chen X, Bian G *et al*. Proteolytic processing, deubiquitinase and interferon antagonist activities of Middle East respiratory syndrome coronavirus papain-like protease. *J Gen Virol* 2014; **95**: 614–626.
- Chu H, Zhou J, Wong BH *et al*. Productive replication of Middle East respiratory syndrome coronavirus in monocyte-derived dendritic cells modulates innate immune response. *Virology* 2014; **454-455**: 197–205.
- Yoneyama M, Kikuchi M, Natsukawa T *et al*. The RNA helicase RIG-I has an essential function in double-stranded RNA-induced innate antiviral responses. *Nat Immunol* 2004; **5**: 730–737.
- Kato H, Sato S, Yoneyama M *et al*. Cell type-specific involvement of RIG-I in antiviral response. *Immunity* 2005; **23**: 19–28.
- Siu KL, Kok KH, Ng MH *et al*. Severe acute respiratory syndrome coronavirus M protein inhibits type I interferon production by impeding the formation of TRAF3-TANK-TBK1/IKK $\epsilon$  complex. *J Biol Chem* 2009; **284**: 16202–16209.
- Neuman BW, Kiss G, Kunding AH *et al*. A structural analysis of M protein in coronavirus assembly and morphology. *J Struct Biol* 2011; **174**: 11–22.
- Siu KL, Chan CP, Kok KH, Woo PCY, Jin DY. Suppression of innate antiviral response by severe acute respiratory syndrome coronavirus M protein is mediated through the first transmembrane domain. *Cell Mol Immunol* 2014; **11**: 141–149.
- Doyle S, Vaicaya S, O'Connell R *et al*. IRF3 mediates a TLR3/TLR4-specific antiviral gene program. *Immunity* 2002; **17**: 251–263.
- Guo B, Cheng G. Modulation of the interferon antiviral response by the TBK1/IKK $\alpha$  adapter protein TANK. *J Biol Chem* 2007; **282**: 11817–11826.
- Ng MH, Ho TH, Kok KH, Siu KL, Li J, Jin DY. MIP-T3 is a negative regulator of innate type I IFN response. *J Immunol* 2011; **187**: 6473–6482.
- Kok KH, Lui PY, Ng MH, Siu KL, Au SW, Jin DY. The double-stranded RNA-binding protein PACT functions as a cellular activator of RIG-I to facilitate innate antiviral response. *Cell Host Microbe* 2011; **9**: 299–309.
- Chaudhary V, Zhang S, Yuen KS *et al*. Suppression of type I and type III interferon signalling by NSs protein of severe fever-with-thrombocytopenia syndrome virus through inhibition of STAT1 phosphorylation and activation. *J Gen Virol* 2015; **96**: 3204–3211.
- Siu KL, Chan CP, Kok KH, Woo PC, Jin DY. Comparative analysis of the activation of unfolded protein response by spike proteins of severe acute respiratory syndrome coronavirus and human coronavirus HKU1. *Cell Biosci* 2014; **4**: 3.
- Iwamura T, Yoneyama M, Yamaguchi K *et al*. Induction of IRF-3/-7 kinase and NF- $\kappa$ B in response to double-stranded RNA and virus infection: common and unique pathways. *Genes Cells* 2001; **6**: 375–388.
- Kew C, Lui PY, Chan CP *et al*. Suppression of PACT-induced type I interferon production by herpes simplex virus 1 Us11 protein. *J Virol* 2013; **87**: 13141–13149.
- Sievers F, Wilm A, Dineen D *et al*. Fast, scalable generation of high-quality protein multiple sequence alignments using Clustal Omega. *Mol Syst Biol* 2011; **7**: 539.
- Deber CM, Wang C, Liu LP *et al*. TM Finder: a prediction program for transmembrane protein segments using a combination of hydrophobicity and nonpolar phase helicity scales. *Protein Sci* 2001; **10**: 212–219.
- Thanos D, Maniatis T. Virus induction of human IFN $\beta$  gene expression requires the assembly of an enhanceosome. *Cell* 1995; **83**: 1091–1100.
- Seth RB, Sun L, Ea CK, Chen ZJ. Identification and characterization of MAVS, a mitochondrial antiviral signaling protein that activates NF- $\kappa$ B and IRF 3. *Cell* 2005; **122**: 669–682.
- Kawai T, Takahashi K, Sato S *et al*. IPS-1, an adapter triggering RIG-I- and Mda5-mediated type I interferon induction. *Nat Immunol* 2005; **6**: 981–988.
- Xu LG, Wang YY, Han KJ, Li LY, Zhai Z *et al*. VISA is an adapter protein required for virus-triggered IFN- $\beta$  signaling. *Mol Cell* 2005; **19**: 727–740.
- Poock H, Bscheider M, Gross O *et al*. Recognition of RNA virus by RIG-I results in activation of CARD9 and inflammasome signaling for interleukin 1 $\beta$  production. *Nat Immunol* 2010; **11**: 63–69.
- Fitzgerald KA, McWhirter SM, Faia KL *et al*. IKK $\epsilon$  and TBK1 are essential components of the IRF3 signaling pathway. *Nat Immunol* 2003; **4**: 491–496.
- McWhirter SM, Fitzgerald KA, Rosains J, Rowe DC, Golenbock DT, Maniatis T. IFN-regulatory factor 3-dependent gene expression is defective in Tbk1-deficient mouse embryonic fibroblasts. *Proc Natl Acad Sci USA* 2004; **101**: 233–238.
- Sankar S, Chan H, Romanow WJ, Li J, Bates RJ. IKK-i signals through IRF3 and NFkappaB to mediate the production of inflammatory cytokines. *Cell Signal* 2006; **18**: 982–993.
- Liu S, Cai X, Wu J *et al*. Phosphorylation of innate immune adapter proteins MAVS, STING, and TRIF induces IRF3 activation. *Science* 2015; **347**: aad2630.
- Lin R, Heylbroeck C, Pitha PM, Hiscott J. Virus-dependent phosphorylation of the IRF-3 transcription factor regulates nuclear translocation, transactivation potential, and proteasome-mediated degradation. *Mol Cell Biol* 1998; **18**: 2986–2996.
- Saha SK, Pietras EM, He JQ *et al*. Regulation of antiviral responses by a direct and specific interaction between TRAF3 and Cardif. *EMBO J* 2006; **25**: 3257–3263.



- 54 van Zuylen WJ, Doyon P, Clément JF *et al*. Proteomic profiling of the TRAF3 interactome network reveals a new role for the ER-to-Golgi transport compartments in innate immunity. *PLoS Pathog* 2012; **8**: e1002747.
- 55 Chen WH, Du L, Chag SM *et al*. Yeast-expressed recombinant protein of the receptor-binding domain in SARS-CoV spike protein with deglycosylated forms as a SARS vaccine candidate. *Hum Vaccin Immunother* 2014; **10**: 648–658.
- 56 Lu L, Liu Q, Zhu Y *et al*. Structure-based discovery of Middle East respiratory syndrome coronavirus fusion inhibitor. *Nat Commun* 2014; **5**: 3067.
- 57 Ying T, Li H, Lu L, Dimitrov DS, Jiang S. Development of human neutralizing monoclonal antibodies for prevention and therapy of MERS-CoV infections. *Microbes Infect* 2015; **17**: 142–148.
- 58 Tatura AL, Baric RS. SARS coronavirus pathogenesis: host innate immune responses and viral antagonism of interferon. *Curr Opin Virol* 2012; **2**: 264–275.
- 59 Kindler E, Thiel V. To sense or not to sense viral RNA—essentials of coronavirus innate immune evasion. *Curr Opin Microbiol* 2014; **20**: 69–75.
- 60 Wong LYR, Lui PY, Jin DY. A molecular arms race between host innate antiviral response and emerging human coronaviruses. *Viral Sin* 2016; **31**: 12–23.
- 61 Yang Y, Ye F, Zhu N *et al*. Middle East respiratory syndrome coronavirus ORF4b protein inhibits type I interferon production through both cytoplasmic and nuclear targets. *Sci Rep* 2015; **5**: 17554.



This work is licensed under a Creative Commons Attribution 4.0 International License. The images or other third party material in this article are included in the article's Creative Commons license, unless indicated otherwise in the credit line; if the material is not included under the Creative Commons license, users will need to obtain permission from the license holder to reproduce the material. To view a copy of this license, visit <http://creativecommons.org/licenses/by/4.0/>